Main Injector Sextupole Requirements

Rod Gerig
Main Accelerator Department
Fermi National Accelerator Laboratory
July 25, 1990

1 Introduction

In this note the required strengths of the two chromaticity correcting sextupole loops are calculated. The work is not considered complete; therefore a significant portion of this note will describe the program used to produce the resulting sextupole curves, and the assumptions that have been used up to this point. It is intended that the program be straightforward in its application to the problem, and that any modifications to the assumptions made thusfar can be easily incorporated.

2 Algorithms

The equations which model the chromaticity are:

$$\xi_H = \xi_{nat_H} + \frac{299.8}{P}\{aS_F + bS_D + cS_{dip}\}$$

and

$$\xi_V = \xi_{nat_V} + \frac{299.8}{P}\{dS_F + eS_D + fS_{dip}\}$$

Where S_F and S_D are the strengths of the chromaticity sextupole in units of $(kg/m^2) - m$ (not B'') and S_{dip} is the sextupole content of the dipoles (using the same units). The coefficints a, b, c, d, e, f, are the chromatic sensitivity coefficients to the changes in the corresponding devices. ξ_{nat_H} and ξ_{nat_V} are the natural chromaticities of the machine, and P is the momentum in GeV/c.

3 Assignment of Sensitivity Coefficients

Although the current lattice is MI_15, the modeling of the Main Injector was done with MI_14. It is believed that this does not make a big difference in the results although it should be looked at.

The sextupole configuration is the one which I have used in all of my tracking studies. It has not been widely publicized, so I will mention it here. All fifty six cells have a sextupole at each

quad. The rf insertions have sextupoles at each quad in the dispersion suppressing half cells, but not in the empty cells where the dispersion is zero. The transfer insertions have sextupoles at the quadrupoles in the adjacent half cells, and at the matching quads, there are sextupoles on the vertical loop. The numbers implied by this scheme are listed below.

Table 1: Sextupole count used in Determining Sensitivity Coefficients

Beamline Section	Number of H Sextupoles	Number of V Sextupoles	Number of Beamline Sections	Total H	Total V
Standard Cell	1	1	56	56	56
rf Insertion	4	4	2	8	8
Transfer Insertion	3	4	6	18	24
ML15 (Total)				82	88

The four sensitivity coefficients corresponding to the sextupole correctors were found using both TEVLAT and SYNCH. The coefficients for the dipoles was found with TEVLAT. The values determined by these programs, and used in my program are:

Table 2: Sensitivity Coefficients

	SYNCH	TEVLAT	Simple FODO	Used in Program
a	.1122	.1104	.131	.111
b	.0174	.0173	.0146	.0174
c		.1686	.179	.1686
d	-.0283	-.0282	-.0265	-.0283
e	-.0653	-.0646	-.0725	-.0653
f		-.1621	-.1628	-.1621

This section seems like the appropriate place to mention the natural chromaticities used; ξ_{nat_H} is -27.5, and ξ_{nat_V} is -28.4.

4 Sextupole Content of Dipoles

I have used three components of sextupole in the dipoles.

$$S_{dip} = S_{remanent} + S_{eddy} + S_{saturation}$$

For the remanent sextupole I used a constant value of

$$1.64\,(kg/m^2) - m$$

This is added at all energies. Its value comes from existing Main Ring multipole measurements on B2 style dipoles.

The eddy current term is proportional to $\dot{P}$. As of this time I have only used the results of Steve Holmes calculation in which he finds an eddy current sextupole of $.24\,T/m^2$ with a ramp rate of $240\,GeV/sec$ [1] . I have converted this to $14.57\,(kg/m^2) - m$ for each dipole at the same ramp rate.

The saturation sextupole calculation is based on Stan Snowdon's note MI-800. On page 4, a table of sextupole content as a function of field is presented. For all practical purposes, only the highest three entries are of any use. I fit these three points to the following equation:

$$S_{units} = \frac{(B - 7.82)^4}{974}$$

and for any field less than 7.82 *kg*, the saturation sextupole is set to zero. Note that this expression is in units; it is converted to $(kg/m^2) - m$ before being added to the other sextupole terms.

5 Ramp Specification

In writing this program I wanted generality, but I did not want to take the time to write a high level ramp specification tool (along the lines of what a console program might have). Thus I borrow the console format, but do not provide the high level entry tools. For instance, if you want to add a slot in the middle of the parabola, you must calculate the time, momemtum and $\dot{P}$ by hand before entering them. A sample ramp file appears below.

```
  time      P     Pdot     Pddot      Cx      Cy


    .1,   8.9,    0.0,      0.00, -10.0, -10.0
  .172,  9.62,   20.0,    277.78, -10.0, -10.0
   .28, 15.02,   80.0,    556.56, -10.0, -10.0
  .312,18.149,115.57,   1111.60, -10.0, -10.0
  .330,20.409,135.58,   1111.60,  10.0,  10.0
.42394, 38.05, 240.0,   1111.60,  10.0,  10.0
 .5654, 72.0 , 240.0,      0.0 ,  10.0,  10.0
.68984, 100.0, 210.0,   -241.07,  10.0,  10.0
.76984, 116.0, 190.0,   -250.0 ,  10.0,  10.0
.81195, 120.0,   0.0, -4512.5 ,  10.0,  10.0
    .9, 120.0,   0.0,      0.0 ,  10.0,  10.0
```

The columns labeled Cx and Cy are not formally a part of the ramp specification, but are the requested chromaticites at those energies. The program linearly interpolates to determine the chromaticity to which it is correcting.

[1] In versions of this note written before 7/24/90 I used the wrong value for the eddy current sextupole. See appendix C.

6 Miscellaneous

Having the above information, the program proceeds to solve the first set of equations for S_F and S_D. The time resolution is presently set to 3 milliseconds. Output is written to an intermediate file and the program "mongo" is used to make the plots.

The program and its supporting files are in:

/home/quad/rod/micalc on the cartoon domain

Source file:	sext_calc.f
Mongo command file:	mongo_sext.com
Ramp files:	ramp*

7 Results

A number of graphs are included with note. More will be forthcoming as our understanding of the magnets increases and as we move into more of an engineering design phase (where sextupole power supply currents and voltages will be of interest). Figures 1 through 5 use a 150 GeV ramp with an unrealistic final parabola. Five different chromaticity curves are represented. The maximum sextupole strengths which appear in these plots is for the case where both chromaticites are -20 units before transition and $+20$ units after transition. In this case the maximum horizontal sextupole strength is $450(kg/m^2) - m$ and comes from the saturation sextupole. The maximum vertical sextupole strength is $-411(kg/m^2) - m$ and it is driven by the eddy current sextupole. It is also clear from these plots that, although it is tempting to suggest that unipolar supplies might be adaquate, the MI will need to have bipolar supplies.

Figure 6 uses a more realistic ramp with a slower $\dot{P}$ near flattop. Although the vertical sextupole is slightly less $(-403(kg/m^2) - m)$, there is no significant change.

Appendicies

A MI_15 Updates

New sensitivity coefficients have been derived for MI_15. The reason they are different from the MI_14 coefficients is not so much due to a change in the lattice, but a realization that the MI_15 design with the quadrupole centered in the ministraight allows more elements to be close to the quadrupole where the lattice functions are closer to the extrema. This uses all elements more effectively. Thus the lattice location for the sextupoles (which are zero-length elements in the models) has been moved to a point .45 meters downstream from the edge of the quadrupole. This in fact could be made closer as the engineering of these ministraights is better understood. The corresponding coefficients are:

Table A-1: Sensitivity Coefficients Revised for MI_15

	Used in Program
a	.1175
b	.0165
c	
d	-.0274
e	-.0666
f	

Figure A-1 shows the sextupole waveforms for the same ramp as in Figure 6. The maximum required strengths are now $425(kg/m^2) - m$ for the sextupoles at focusing quads and $-386(kg/m^2) - m$ for the sextupoles at vertical quads.

In configuring the sextupoles, twelve S_D sextupoles had been placed around the long straight sections. This was done because of my concern about the lesser effect of the S_D loop on chromaticity. However, this more complete analysis has shown that the S_D loop does not need to be as strong as the S_F loop. The sextupoles around the long straight sections may interfere with external beamlines, so there is motivation to get by without them. The sensitivity coefficients for the S_D sextupoles have been recalculated with only 76 rather than 88 sextupoles. The results are:

Table A-2: Sensitivity Coefficients for 76 S_D Sextupoles: MI_15

b	.0142
e	-.0614

Figure A-2 indicates the needed sextupole strengths for this configuration. The maximum required strengths are $423(kg/m^2) - m$ for the sextupoles at focusing quads and $-417(kg/m^2) - m$ for the S_D sextupoles.

Appendix B

B Standard Ramp

Phil Martin has released MI note 27 in which he specifies a standard ramp for the Main Injector. It differs from the other ramps shown in this note in that it only goes to 120 GeV/c, and it only has one parabola time constant prior to linear acceleration. The effect of this ramp on the sextupoles is shown in Figure B-1. The most notable feature of this change is that the maximum eddy current sextupole has moved earlier and now occurs at a momentum of 19.8 GeV/c where as before it occured at 26 GeV/c. The magnitude is also greater; 8.1 units (at an inch) as opposed to 6.7 units.

Appendix C

C Corrections

I must include this appendix to admit that the results presented with regard to eddy current sextupole are incorrect. The number which I had previously used, $3.1G/in^2$ is actually a B". Thus the eddy current sextupole reported up until now is twice the actual size. Figures A-2 and B-1 have been redone but the orignal Figures A-2 and B-1 are still in the report so that the differences can be seen. Older Figures are not recalculated. The greatest effect of this change is on the sextupole content of dipole in the parabola. A smaller effect is on the needed strength of the vertical sextupole loop. It can be seen (Figure A-2) that the maximum strength of the vertical sextupoles is reduced from $-417(kg/m^2) - m$ to $-394(kg/m^2) - m$.

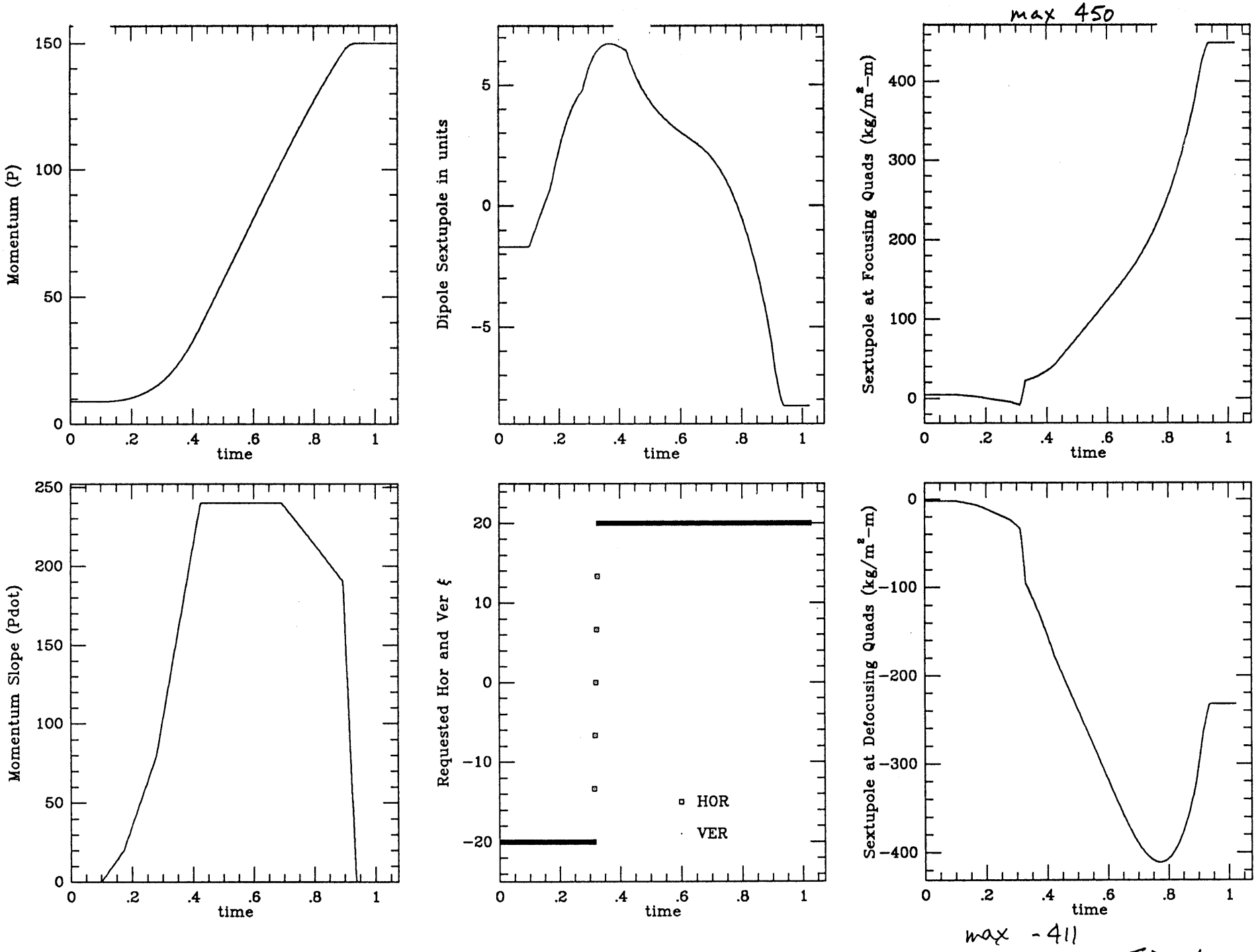

Main Injector 150 gev Ramp

Fig 1

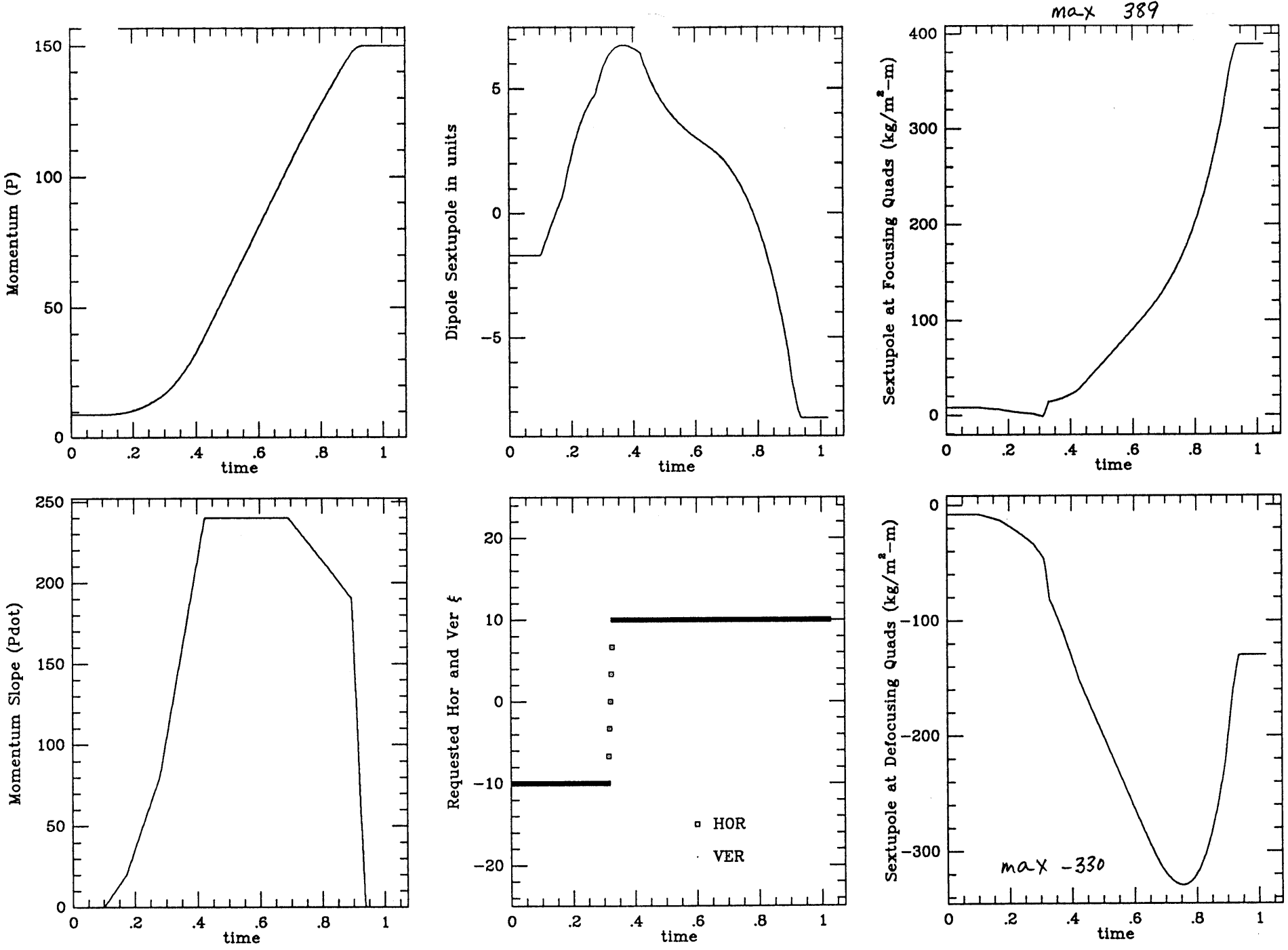

Main Injector 150 gev Ramp

Figure 2

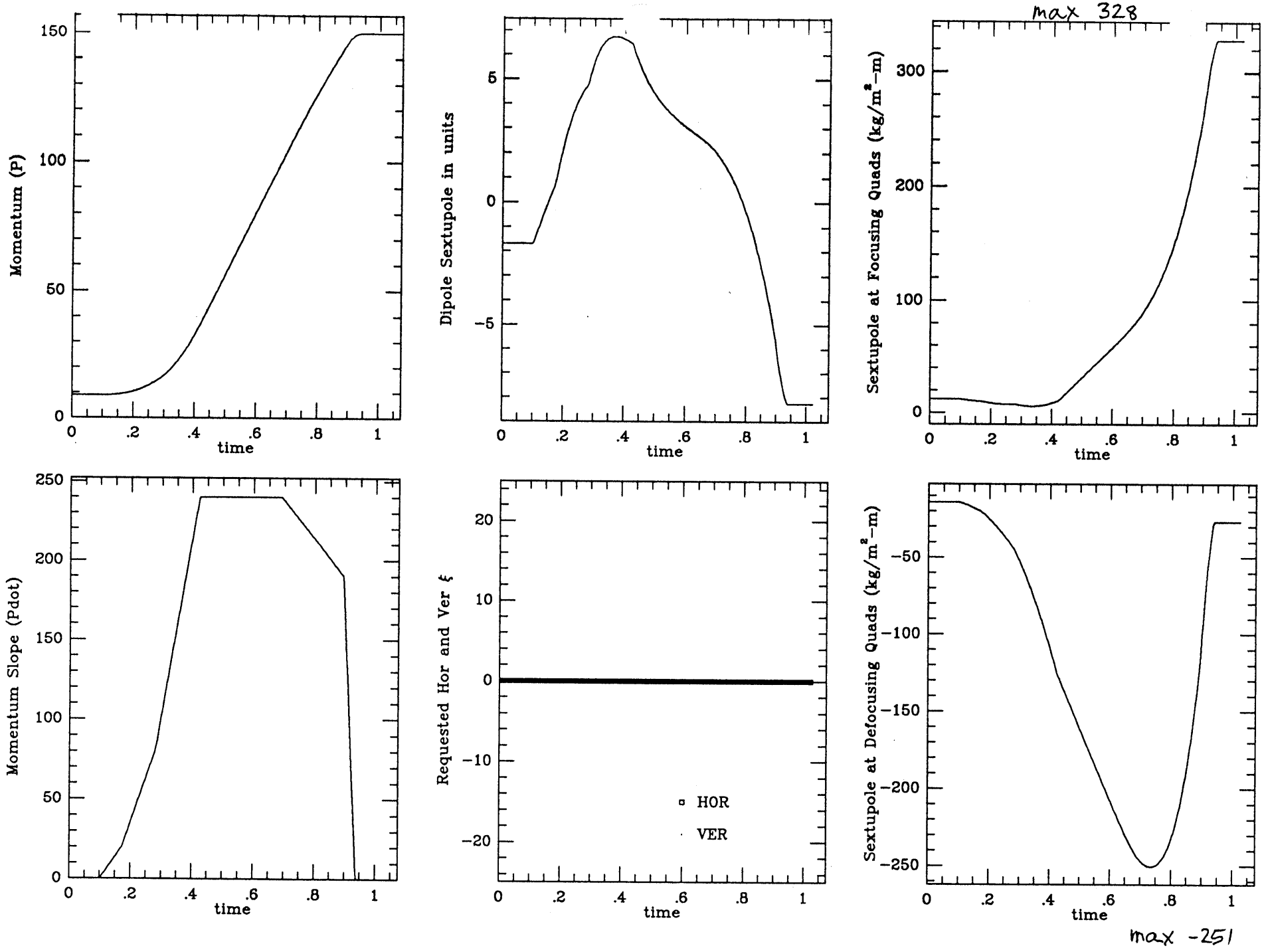

Main Injector 150 gev Ramp

Figure 3

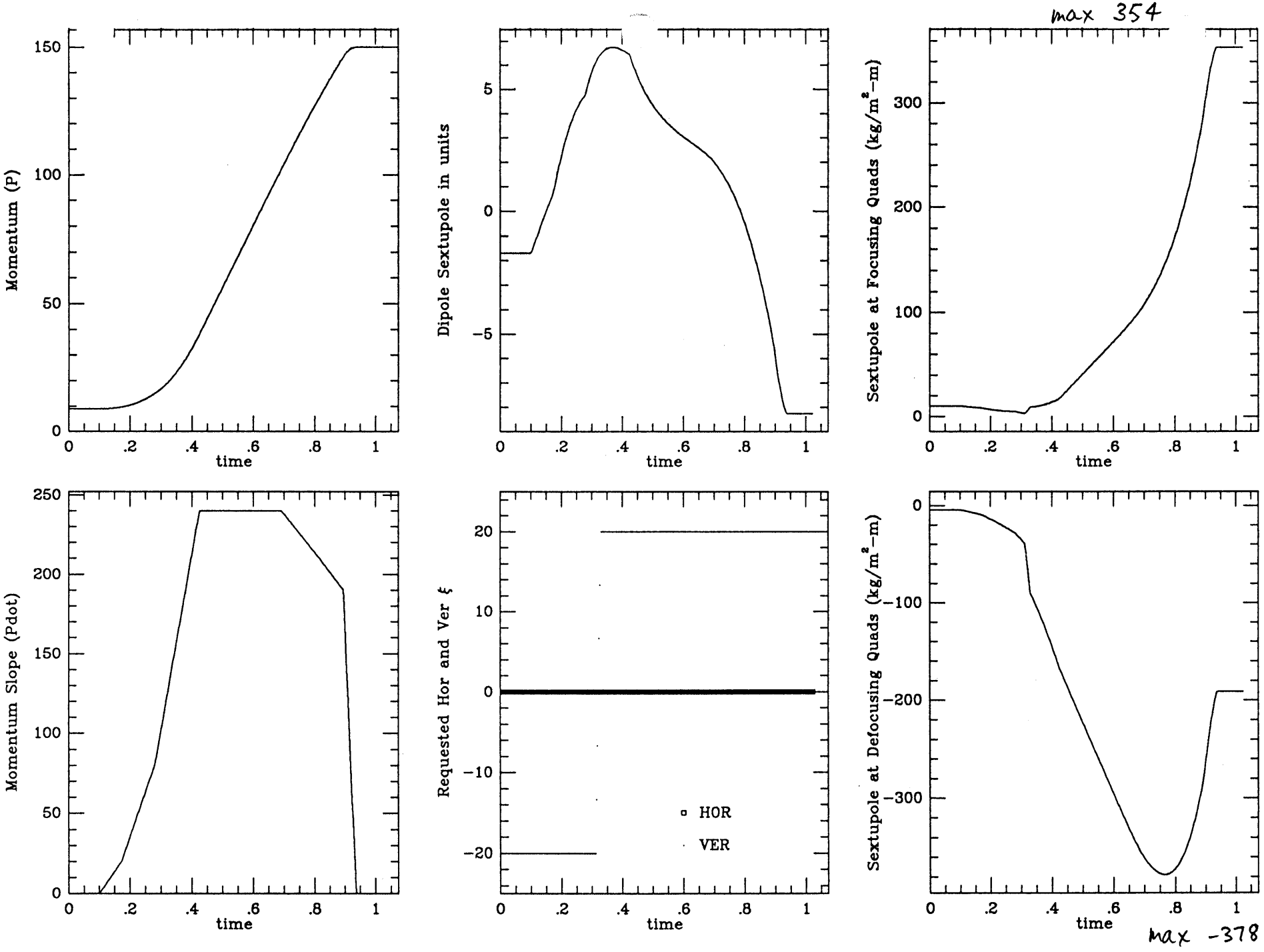

Main Injector 150 gev Ramp

Fig 4

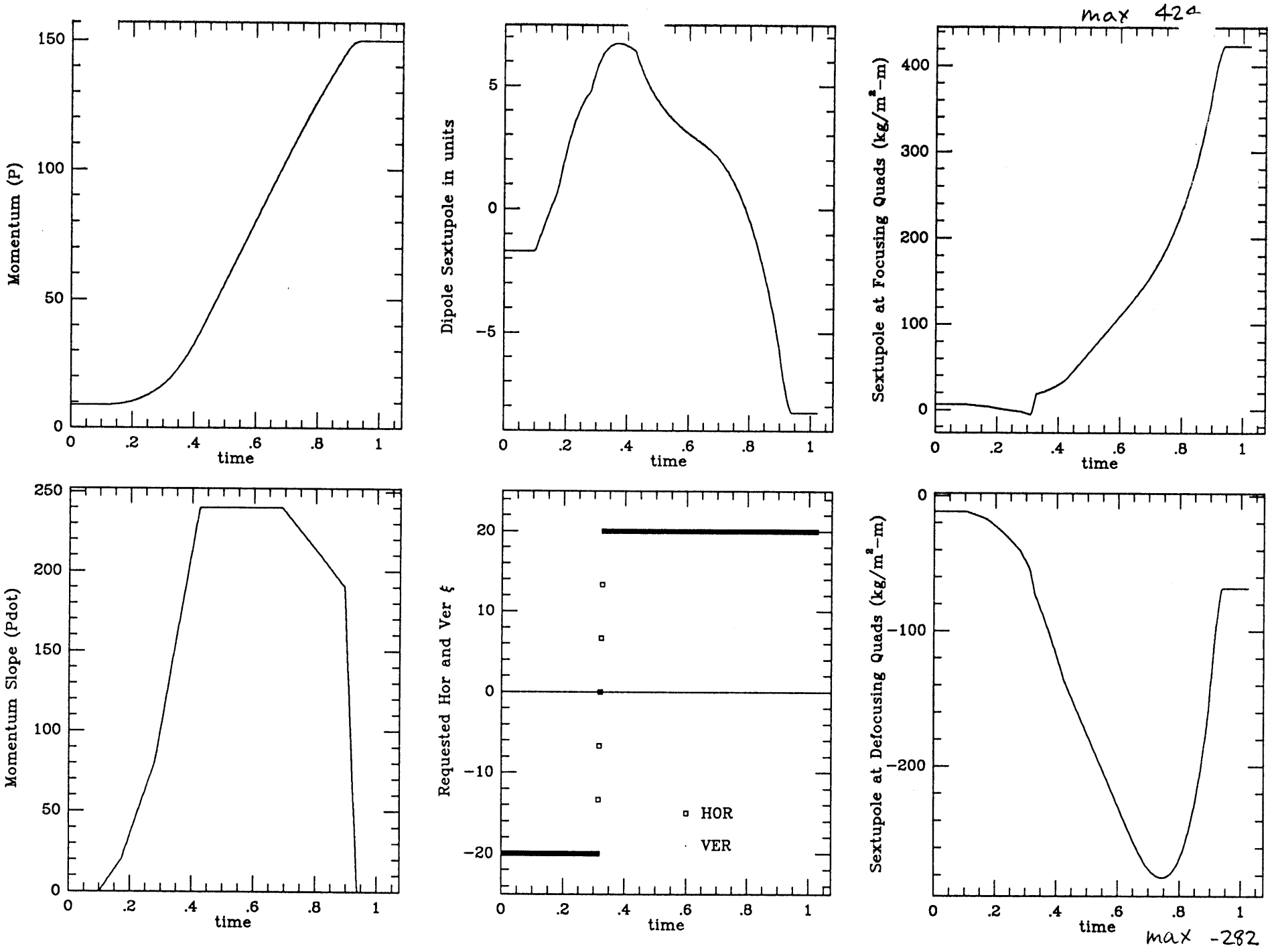

Main Injector 150 gev Ramp

Figure 5

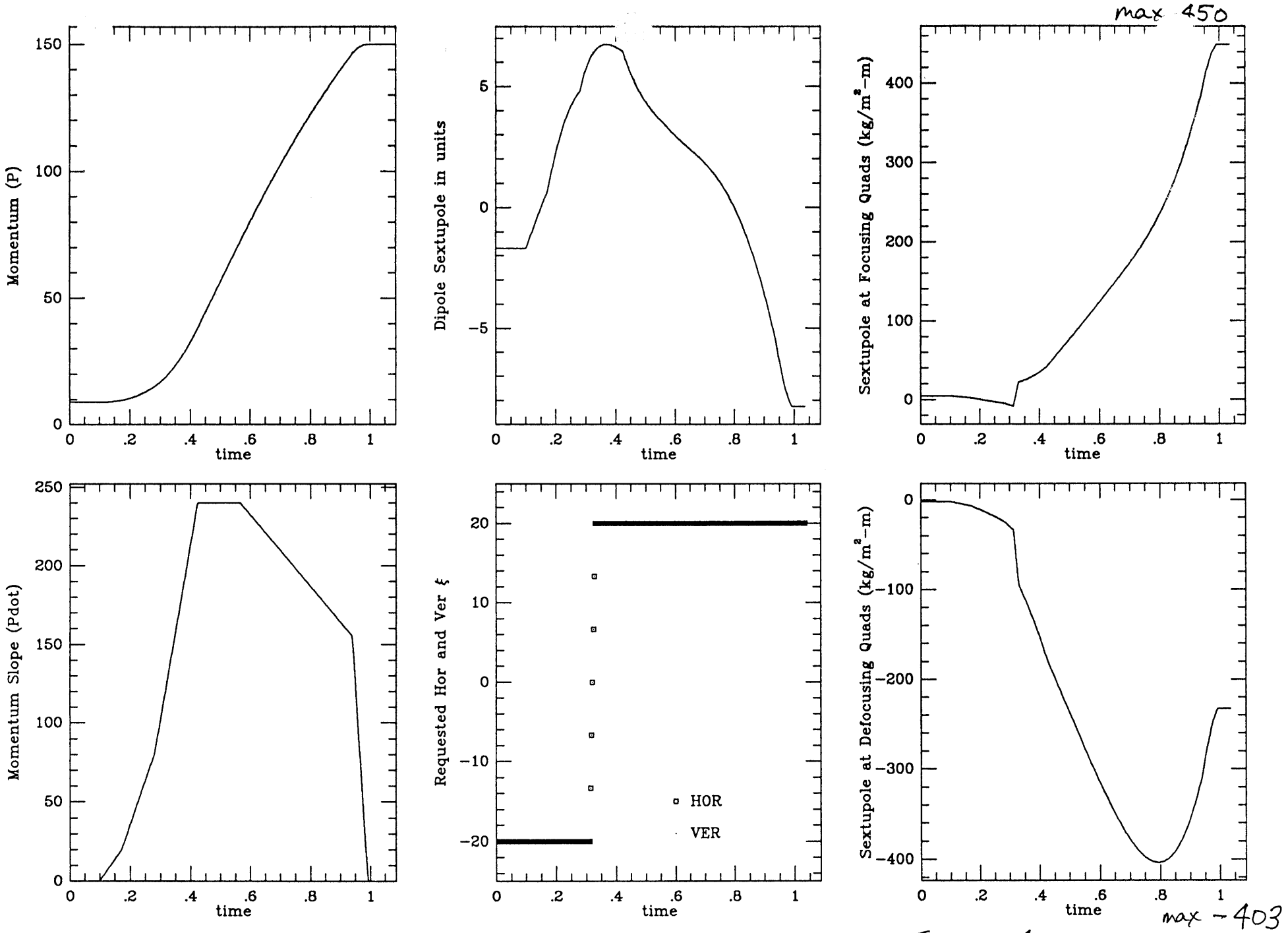

Figure 6

MI 150 Gev Ramp (slower pdot near flattop)

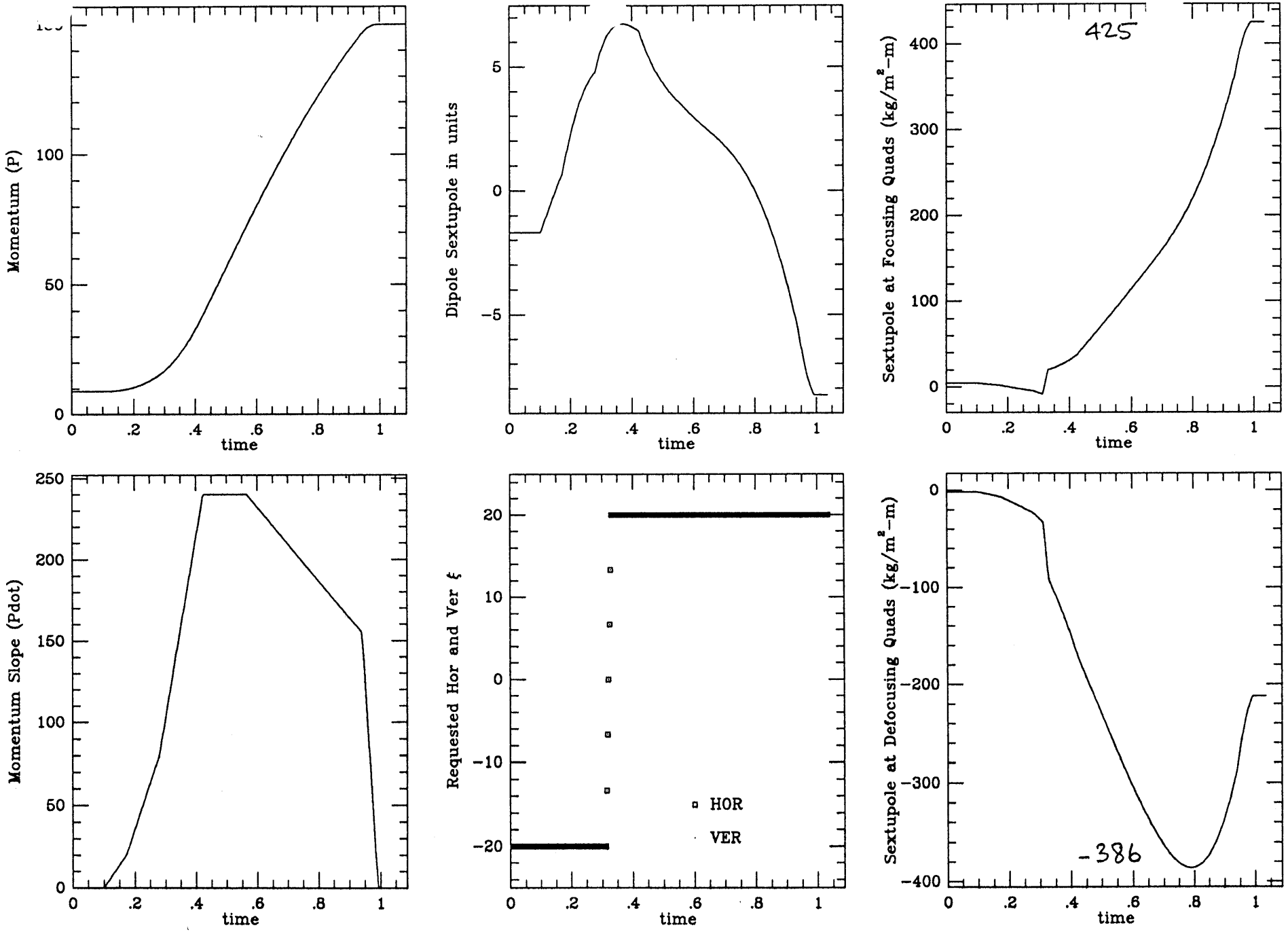

mi_15 coefficients

Figure A-1

MI 150 Gev Ramp (slower pdot near flattop)

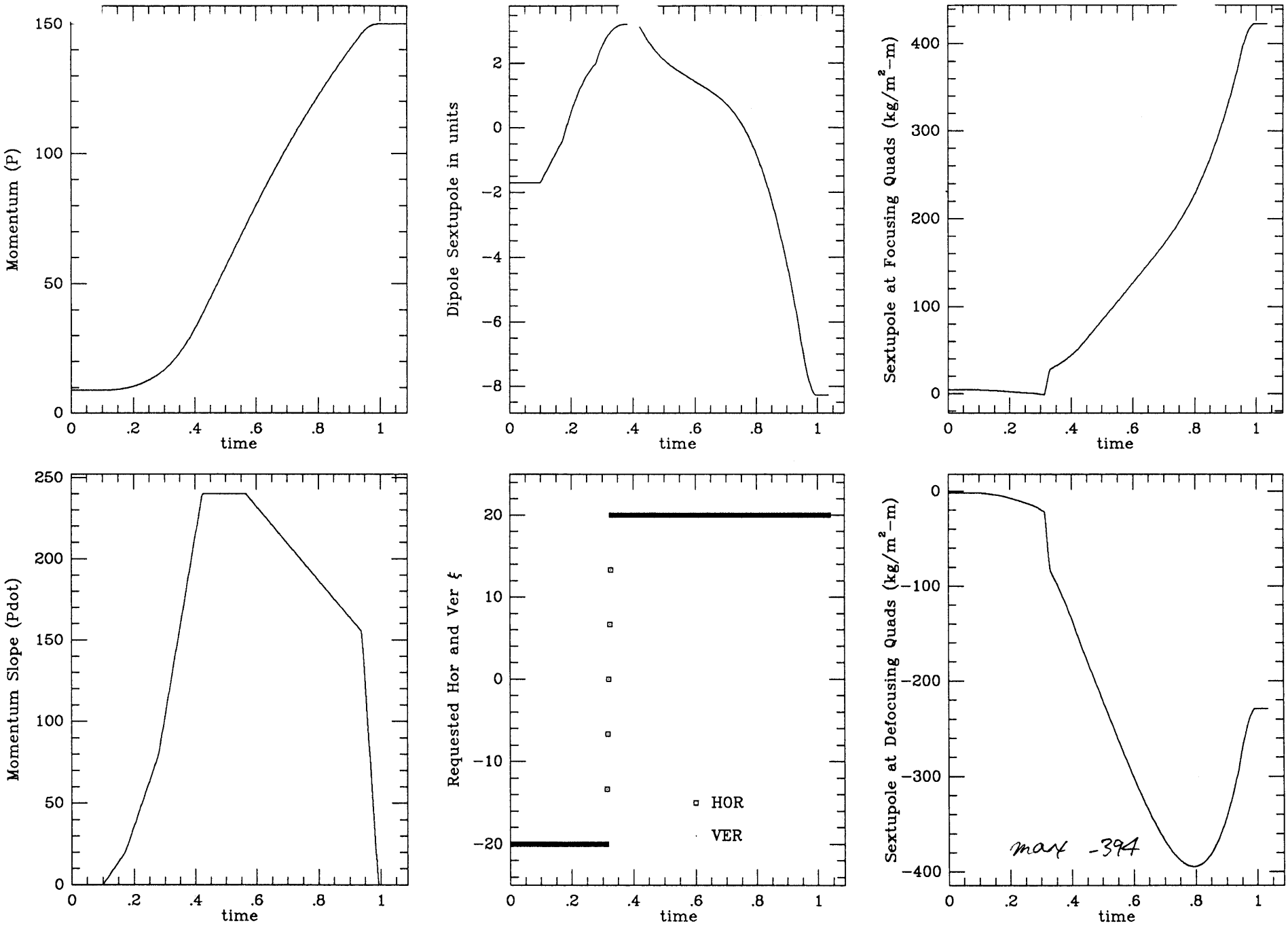

MI 150 GeV Ramp (slower pdot near flattop)

Revised Figure 4-2

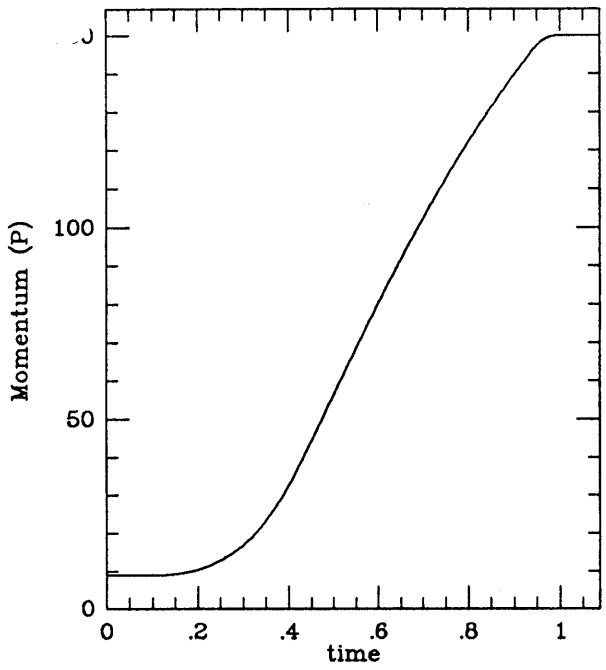

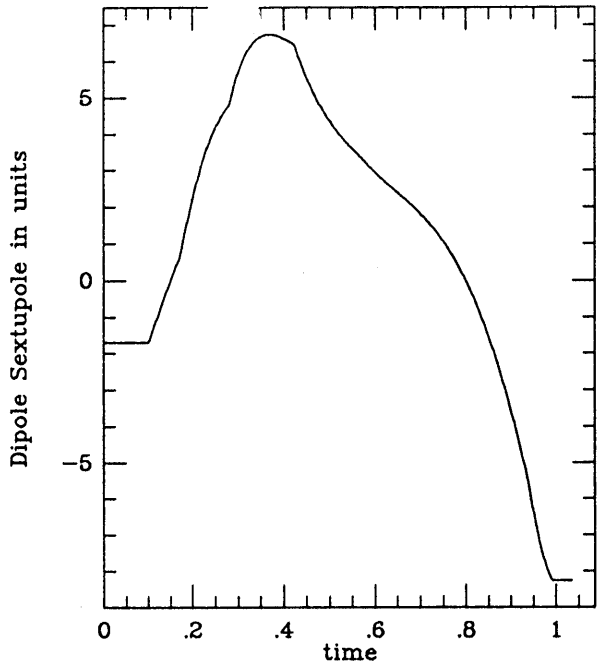

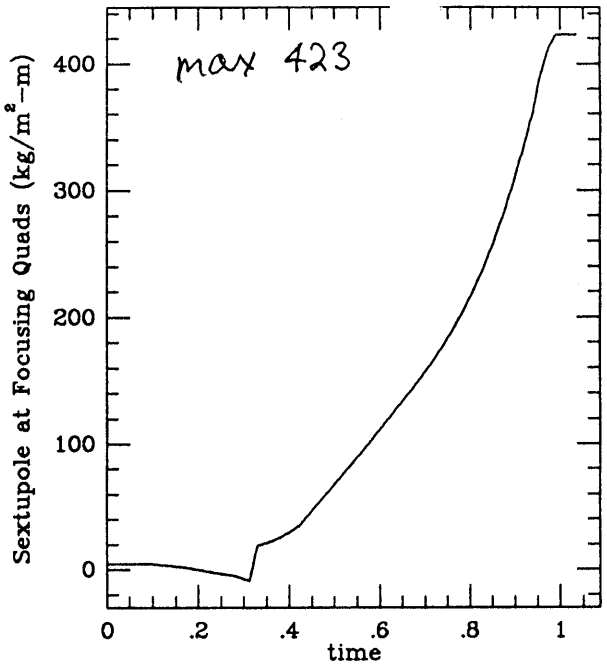

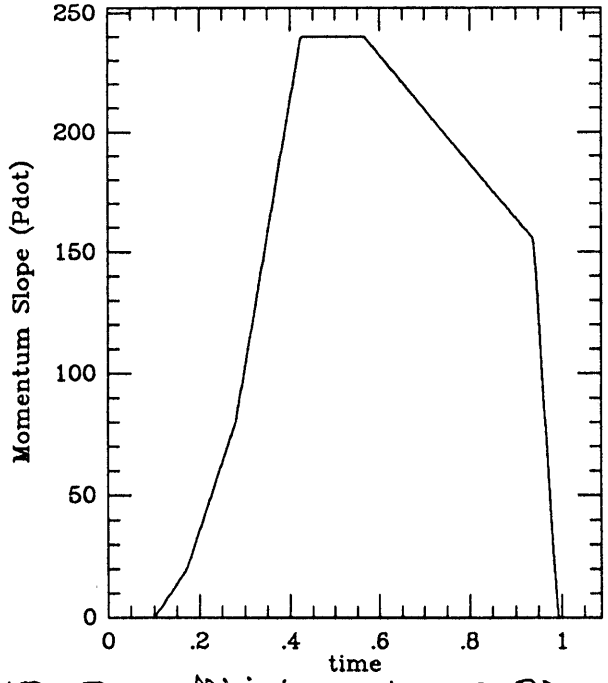

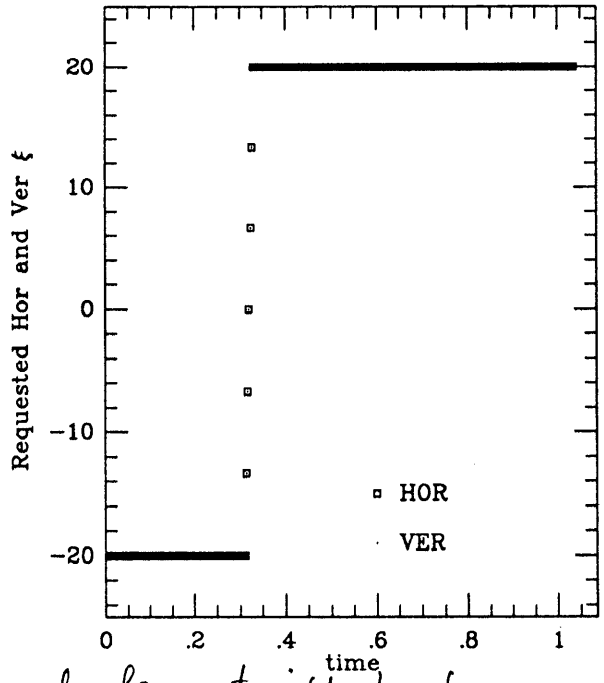

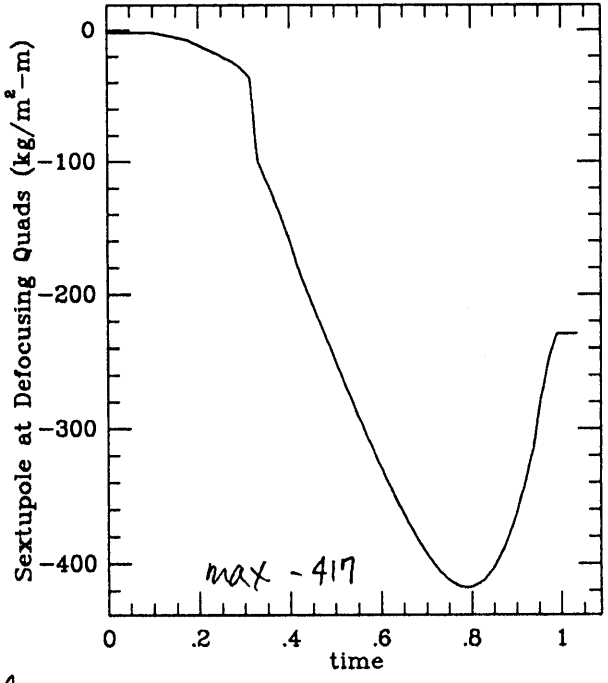

MI-15 coefficients, the 12 SDs around long straight have been removed

MI 150 Gev Ramp (slower pdot near flattop)

FIGURE 1-2

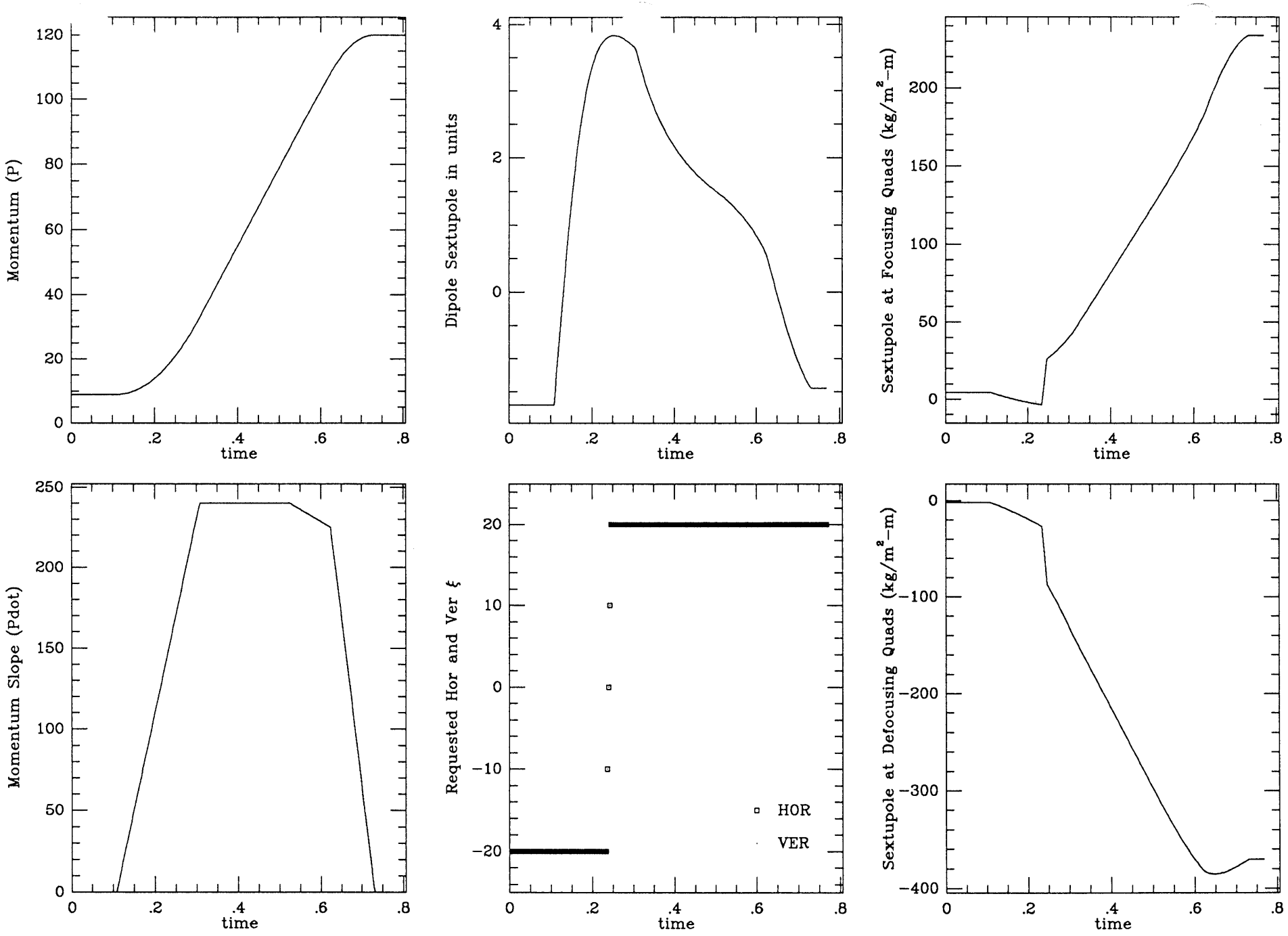

MI 120 Gev Ramp from MI Note 27

Revised Figure B-1

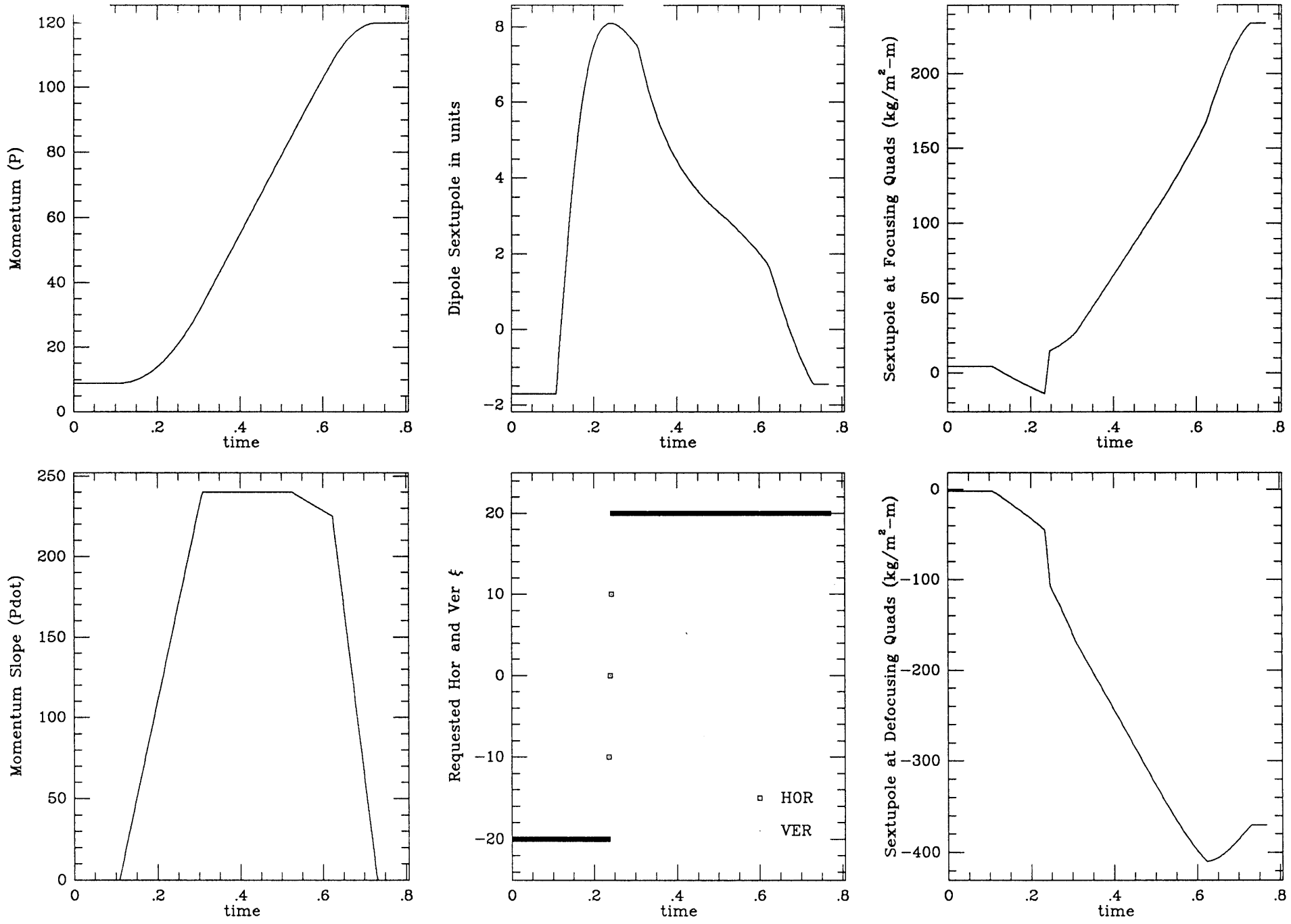

MI 120 Gev Ramp from MI Note 27

Figure B-1